

## **FIRE PERFORMANCE OF CONCRETE BEAMS REINFORCED WITH FRP BARS**

Ali Nadjai<sup>1</sup>, Didier Talamona<sup>1</sup>, Faris Ali<sup>1</sup>

<sup>1</sup>University of Ulster, School of the Built Environment, FireSERT Block 27,  
Shore Road, Jordanstown, Belfast, Co Antrim, BT37 0QB  
E-mail: a.nadjai@ulster.ac.uk

### **ABSTRACT**

The fire resistance of concrete members reinforced with fibre reinforced polymer (FRP) rebars is extremely crucial area that needs to be investigated prior to implementing FRP composite materials in buildings. This work analyses the structural behaviour of concrete beams reinforced with hybrid FRP and steel reinforcements at elevated temperatures. The slice approach model was used and validated against experimental data for reinforced concrete beams with FRP available in the literature. Good agreement with experimental results has been obtained at room temperature as well as at elevated temperatures.

### **KEYWORDS**

FRP, RC Beams, Fire, approach method

### **INTRODUCTION**

Worldwide interest in the use of Fibre Reinforced Polymer (FRP) reinforcement in concrete structures as an alternative to a traditional structural material such as steel reinforcement has increased significantly in recent years. FRP reinforcement has an advantage over steel in that it has high corrosion resistance and a high strength to weight ratio. For example, in the UK and European Union countries alone, the annual cost of repair and maintenance of the infrastructure, as a result of problems associated with corrosion, is around £20 billion [1]. Most existing solutions for the improvement of structural durability are expensive or complicate initial construction. It is generally expected that the use of FRP rebars, as opposed to steel, will reduce these maintenance costs by over 80% in the long-term [1]. Furthermore, the use of composites in the rehabilitation of existing structures reduces the overall costs (including time for execution) by over 25%.

While FRP reinforcement is mainly used in bridges, there is enormous economic potential for its use in multi-storey buildings, parking garages and industrial structures. However, before FRP can be used to reinforce concrete members in buildings, the stability of these members to meet stringent fire resistance requirements must be established. Although it was found that the behaviour of FRP reinforced concrete structures at ambient temperatures is satisfactory [2- 13] information regarding the behaviour of FRP reinforced concrete members at high temperatures is still lacking. The behaviour of FRP bar reinforced concrete under fire exposure is quite different from conventional steel reinforced concrete. When embedded in concrete, the lack of oxygen will inhibit the burning of FRP reinforcement, but the resin will soften. The critical time will occur when the resin on the surface of the FRP bar reaches its glass transition temperature. At this point, the resin will no longer be able to transfer stresses from the concrete to the fibre, i.e. the bond will fail. Locally this may result in increased crack width hence increased deflections. Collapse will occur when the temperature of the fibre reaches the level at which it starts to degrade. The fire resistance of concrete reinforced with FRP rebars depends on the change in mechanical properties of FRP and concrete due to fire exposure. The effect of fire on the mechanical properties of concrete is well documented where it has been shown that high temperature decreases the modulus of elasticity and the compressive strength of concrete. A serious matter relating to the use of FRP's in structural applications is the lack of design codes and specifications. However, data of the effect of high temperatures on the FRP is limited. The behaviour of these composites when subjected to fire is complex and not sufficiently well understood.

## TIMELINESS AND NOVELTY

There is a clear need for improved understanding of the performance of materials in fire to ensure adequate levels of safety and to provide clear design guidance, and produce cost-effective design solutions. Within the past 10 years sophisticated computer programs have been developed to model the behaviour of concrete frames in fire. In some respects these programs are still inadequately validated because of the sparseness of relevant input data. In particular, very few experimentally obtained input fire data is available on the behaviour of composite beams reinforced with FRP bars [14, 15]. The FRP bar's characteristic material behaviour is linear up to failure. This property makes its structural behaviour brittle, and the concrete becomes the ductile component (by crushing of concrete) of reinforced concrete structures (Figure 1). The design criterion of flexural beams, consequently, has to be based on the achievement of concrete failure (over-reinforced beams) providing a reinforcement percentage ratio higher than that corresponding to the balanced failure. Besides, the low elastic modulus of FRP's results in high deformability, lack of ductility, and high crack widths. Consequently the design criterion for FRP reinforced concrete structures shifts to the serviceability limit states that check the structural behaviour aspect instead of the strength to ensure functionality and safety during the expected life of the structures

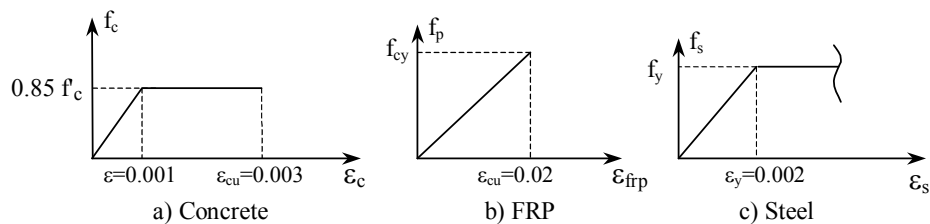


Figure 1. Flexural Stress-strain relations

An improvement in the structural performances of concrete beams can be obtained using a combination of FRP and steel reinforcement or, alternatively, FRP bars manufactured combining two or more different reinforcing fibres (hybrid FRP bars). In both cases, it is possible to design beams with an adequate level of ductility, ensuring good durability. Hybrid FRP bars present bilinear ductility stress-strain behaviour. At present, different types of hybrid FRP bars are available, even if they have shown limited practical developments. On the other hand, a combination of FRP and steel reinforcement seems to be a practical and effective design solution for concrete beams subjected to fire situations.

## EFFECT OF FIRE ON THE CONCRETE STRENGTH

Initially, the heat applied to concrete beams causes evaporation of free moisture in the concrete. With a continued exposure to fire, the temperature inside the beam increases and the strength of concrete decreases. In certain cases, the pressure generated by conversion of moisture within beams may be too high for the surface layer of concrete to resist, and it may spall causing a reduction in concrete compressive strength. This reduction in the compressive concrete strength at high temperatures has been taken into consideration in most existing design codes. For the purposes of a general design method proposed in this paper, values of reduced strength of concrete  $f_{cuT}$  due to the fire exposure are derived as given below, from rules given in the ENV EC2 Part1.2 [16].

According to ENV EC2 Part 1.2, reduction in strength of steel corresponds to the various conditions of using and specifying its strength. The values of reduced strength and modulus of elasticity of reinforcing steel ( $f_{yT}$  and  $E_T$ ) given below, apply to the common grade of steel which was used in beams for testing, as reported later in this paper:

$$f_{cuT} / f_{cu} = k_c \quad (1)$$

$$k_c = 1.0 \quad \text{for } T \leq 100 \text{ (T in } ^\circ\text{C)}$$

$$k_c = (1.067 - 0.00067T) \quad \text{for } 100 \leq T \leq 400$$

$$k_c = (1.44 - 0.167T) \quad \text{for } 400 \leq T \leq 900$$

$$k_c = 0 \quad \text{for } 900 \leq T$$

$$f_{yT}/f_{yv} = k_s \quad (2)$$

$$k_s = 1.0 \quad \text{for } T \leq 350$$

$$k_s = (1.899 - 0.00257T) \quad \text{for } 350 \leq T \leq 700$$

$$k_s = (0.24 - 0.0002T) \quad \text{for } 700 \leq T \leq 1200$$

$$k_s = 0 \quad \text{for } 1200 \leq T$$

$$E_T/E_{20} = k_c \quad (3)$$

$$K_c = 1.0 \quad \text{for } T \leq 100$$

$$K_c = (1.10 - 0.001T) \quad \text{for } 100 \leq T \leq 500$$

$$K_c = (2.05 - 0.0029T) \quad \text{for } 500 \leq T \leq 600$$

$$K_c = (1.39 - 0.0018T) \quad \text{for } 600 \leq T \leq 700$$

$$K_c = (0.41 - 0.0004T) \quad \text{for } 700 \leq T \leq 800$$

$$K_c = (0.27 - 0.000225T) \quad \text{for } 800 \leq T \leq 1200$$

$$K_c = 0 \quad \text{for } 1200 \leq T$$

### EFFECT OF FIRE EXPOSURE ON FRP's MECHANICAL PROPERTIES

The reduction in mechanical properties of FRP due to high temperature depends mainly on the specific composition and properties of the matrix and reinforcing fibres. The structure role of the matrix, which is to hold the reinforcing fibres in place and transfer stresses among them, may be compromised as the temperature of the composite approaches the glass transition temperature  $T_g$  of the polymer. The result, is that the composite loses its tensile strength and stiffness. The failure of the composite occurs when the temperature of the fibres themselves reaches the level at which they start to degrade, which will be in the region of  $600^{\circ}\text{C}$  for glass and significantly higher for carbon. An extensive survey done by Blontrok et al. [17] on the effect of high temperature on the mechanical properties of FRP rebars showed that although the experimental results were scattered, the ultimate tensile strength of AFRP and CFRP rebars was not affected by heat up to  $100^{\circ}\text{C}$ , however, it decreases dramatically with increasing the temperature. The tensile strength of GFRP rebars, however, decreases consistently with the increase of the temperature. The modulus of elasticity of three FRP rebars was constant up to  $100^{\circ}\text{C}$ , and then decreased linearly with increases in the temperature. Based on the experimental results collected by Blontrok et al. [17], the values of reduced ultimate tensile strength and modulus of elasticity of FRP rebars due to the temperature can be obtained from the following proposed conservative equations:

$$\frac{f_{fuT}}{f_{fu20}} = k_f \quad (4) \quad \text{and} \quad \frac{E_{fT}}{E_{f20}} = k_E \quad (5)$$

Where  $f_{fu20}$  and  $f_{fuT}$  are the ultimate strength of FRP rebars at  $20^{\circ}\text{C}$  and  $T^{\circ}\text{C}$  respectively,  $E_{f20}$  and  $E_{fT}$  are the modulus of elasticity of FRP rebars at  $20^{\circ}\text{C}$  and  $T^{\circ}\text{C}$  respectively, and  $k_f$  and  $k_E$  are temperature reduction factors for the tensile strength and the modulus of elasticity, respectively. The proposed  $k_f$  and  $k_E$  reduction factors as a function of FRP temperatures are shown in Figures 2 and 3. The reduction factors of steel bars are also shown in these figures as proposed by ENV EC2 Part 1.2 [16]. The reduction factors  $k_f$  and  $k_E$  are given as follows:

#### GFRP rebars

$$K_f = (1 - 0.0025T) \quad \text{for } 0 \leq T \leq 400$$

$$K_f = 0 \quad \text{for } 400 \leq T$$

#### AFRP rebars

$K_f = 1$	for $0 \leq T \leq 100$	$K_E = 1$	for $0 \leq T \leq 100$
$K_f = (1.333 - 0.00333T)$	for $100 \leq T \leq 400$	$K_E = (1.25 - 0.0025T)$	for $100 \leq T \leq 300$
$K_f = 0$	for $400 \leq T$	$K_E = (2.0 - 0.005T)$	for $300 \leq T \leq 400$
		$K_E = 0$	for $400 \leq T$

### CFRP rebars

$$K_f = 1 \quad \text{for } 0 \leq T \leq 100$$

$$K_f = (1.267 - 0.00267T) \quad \text{for } 100 \leq T \leq 475$$

$$K_f = 0 \quad \text{for } 475 \leq T$$

$$K_E = 1 \quad \text{for } 0 \leq T \leq 100$$

$$K_E = (1.175 - 0.00175T) \quad \text{for } 100 \leq T \leq 300$$

$$K_E = (1.625 - 0.00325T) \quad \text{for } 300 \leq T \leq 500$$

$$K_E = 0 \quad \text{for } 500 \leq T$$

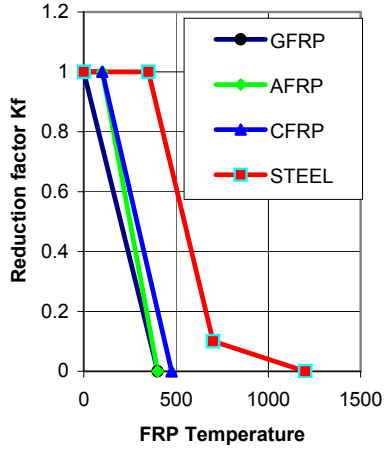


Figure 2. Temperature reduction factor for FRP tensile strength

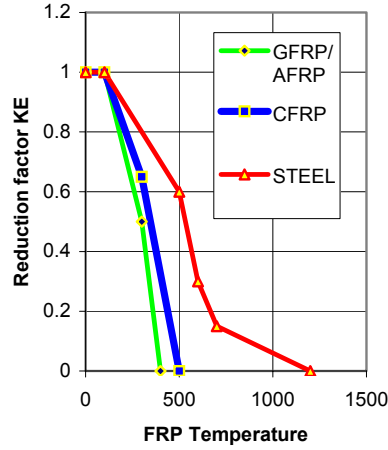


Figure 3. Temperature reduction factor for FRP modulus of elasticity

### TEMPERATURE PROFILE IN FRP REINFORCED RECTANGULAR BEAMS

The rise in temperature inside beams, as a response to its exposure, depends on large number of factors such as the moisture content in concrete and the composition of the cement and aggregate. Also, the development of temperature in a beam depends on the heating conditions and the heat transfer characteristics of the environment. However, these factors cannot be obtained conveniently and used with confidence in any general design rules. Based on test results obtained by Lin [17], Desai [18] developed an equation to predict the temperature profiles in rectangular concrete beams. The temperatures contours are assumed to be parallel to the vertical faces and the soffit of the exposed beam to fire on these three faces. Also, it is assumed that, for a beam exposed to fire on three sides, the following factors govern the temperature ( $T$  °C) inside the beam, along a contour  $x$  mm away from these sides:

- (a) the ambient temperature, a function of the fire exposure period ( $t$ , in min)
- (b)  $b$ , the width of the cross-section (mm) and
- (c)  $r$ , the ratio of the overall height to the width.

Desai's cubic equation, used in this paper is given as follows:

$$T = (D - Ax + Bx^2 - Cx^3)/t^{0.25} \quad (6)$$

The values of A, B, C and D can be obtained as follows:

$$A = 3.33(3 + 0.0033t + \frac{(100-t)}{b})$$

Where:  $B = 0.085$ ,  $C = 0.000221$  and  $D = 475t^{7/12} - (b - 105t^{1/3})$

The application of this method is limited to rectangular beams with width (mm) within the range  $100 \leq b \leq 300$  and values of  $r$  within the range of  $1 \leq r \leq 3$ . Typical temperature contours in a FRP reinforced beam having a width of 200 mm and depth of 300 mm estimated at 90 min as shown in Figure 4.

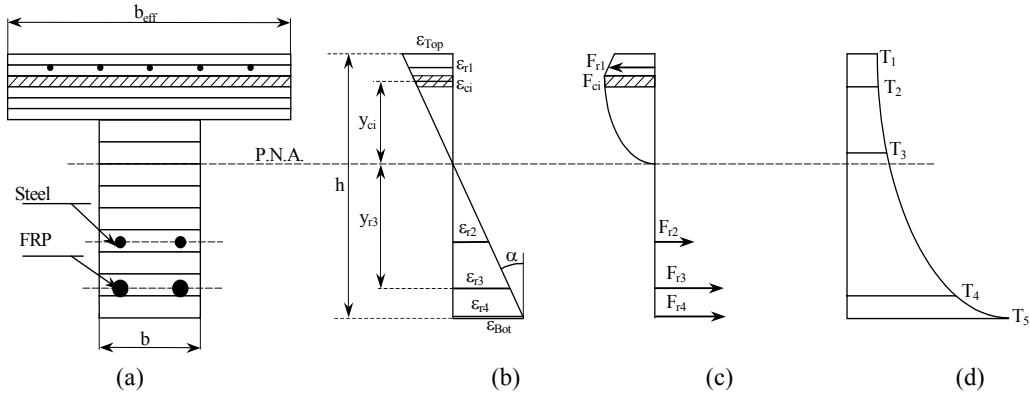


Figure 4: Method of Slices.

### FLEXURAL CAPACITY OF REINFORCED BEAM USING THE SLICES APPROACH

The complexities of material properties are introduced into the analysis of sectional behaviour by means of a method of slices executed by means of a spreadsheet, and the important features of the methodology are illustrated in Figure 4. The cross-section of the beam can be divided up to a maximum of 100 slices (Figure 4(a)), the reinforcement being added separately, reduction in concrete area due to the reinforcement being ignored. Two layers of steel reinforcements and two layers of F.R.P. strengthening can be modelled for each cross-section. The objective is to evaluate the plastic moment capacity of the cross section at each timestep so that the flexural strength history for the duration of the fire event may be plotted. A typical temperature distribution is shown in Figure 4(d).

The temperature through the depth of the section is estimated using a linear interpolation or Lagrange shape function [20]. To establish the temperature distribution the temperature has to be known (via experimental measurement or using simple formulae [19] or tables) at five different locations through the depth. The temperature will be calculated at each centre of gravity of the concrete slices and at the reinforcement location. The material properties are established for each element depending on its temperature. The magnitude of each ultimate plastic moment capacity for each temperature distribution is determined by deriving a moment curvature graph. The process is to define a specific curvature and from that evaluate the associate moment generated in the analytical model. Hence moments are tabulated by repeating calculations over a range of curvatures. The curvature  $\delta\theta/\delta x$  is defined (Figure 4(b)) in terms of a notional maximum fibre strain, which would produce a curvature  $\Phi 2\varepsilon_{\max}/d = (\mu\varepsilon/\text{mm})$  over half the depth of the section.

The equivalent forces are calculated depending on the strain distribution ( $\varepsilon_{\text{Tot}} = \varepsilon_{\text{Top}} + \varepsilon_{\text{Bot}}$ ). If the horizontal equilibrium of the section is not satisfied then the Plastic Neutral Axis (PNA) is moved up or down (using a dichotomy algorithm) depending on the out of balance forces. The new  $\varepsilon_{\text{Top}}$  and  $\varepsilon_{\text{Bot}}$  are calculated until the horizontal equilibrium is reached. Once the equilibrium stage has been reach, the bending moment is established by multiplying each individual force by the arm lever from the application point of this force to the Plastic Neutral Axis. Then the total strain ( $\varepsilon_{\text{Tot}}$ ) is increased until horizontal equilibrium cannot be reached any more (Figure 4) and the program starts new calculations using the temperatures described in the following time steps until it reaches the last time step (up to seven time steps can be defined for each calculation)

### DEFLECTION PREDICTION

The deflection due to flexure at any point on a beam and at any load level can be calculated if the true moment curvature relationship and the bending moment variation for the beam are known. This follows from the following well-known equation of virtual work:

$$\delta_A = \int_0^L \frac{mM}{EI} dx \quad (7) \quad \text{or more generally} \quad \delta_A = \int_0^L m \psi dx \quad (8)$$

where  $\delta$  is the desired deflection of a point A on the beam,  $m$  is the bending moment due to a unit load applied at a point A in the direction of desired deflection,  $M/EI$  or  $\Psi$  is the curvature, and  $L$  is the beam span.

Consider the simply supported beam in Figure 5(a) subjected to two point loads  $P$ . The curvature  $M/EI$  diagram of the beam is illustrated in Figure 5(b), where sections at a distance less than  $L_g$  from the support are considered uncracked because they are subjected to moments less than  $M_{cr}$ .

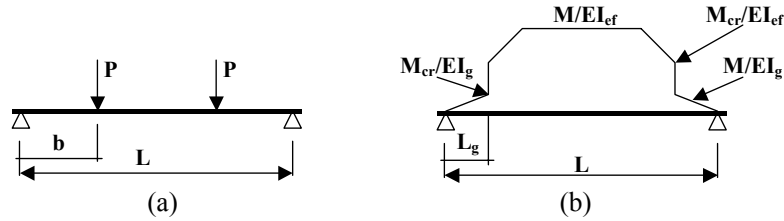


Figure 5. Load and curvature distribution along simply supported beam

For calculation of deflection under the two load  $P$

$$\delta_{uncr} = \frac{PL^3}{6EI_g} \times \left( \frac{3b}{4L} - \frac{b^3}{L^3} \right) \quad \text{for } M < M_{cr} \quad (9)$$

$$\delta = \frac{PL_g^3}{3EI_g} + \left[ \frac{Pb}{EI_{ef}} - \frac{PL_g}{EI_{ef}} \right] \times \left[ \left( \frac{b-L_g}{2} \right) \times \left( \frac{2b+L_g}{3} \right) \right] + \quad \text{for } M_a > M_{cr} \quad (10)$$

$$\left[ \left( \frac{PL_g}{EI_{ef}} \right) \times \left( \frac{L}{2} - L_g \right) \times \left( \frac{L}{4} + \frac{L_g}{2} \right) \right] + \left[ \left( \frac{P(b-L_g)}{EI_{ef}} \right) \times \left( \frac{L}{2} - b \right) \times \left( \frac{L}{4} + \frac{b}{2} \right) \right]$$

Using the well known semi-empirical cubic equation [21] for the effective moment of inertia of the beam  $I_e$  to compute the deflection after cracking for unstrengthened reinforced concrete beams.

$$I_e = \left( \frac{M_{cr}}{M_a} \right)^3 I_g + \left\{ 1 - \left( \frac{M_{cr}}{M_a} \right)^3 \right\} I_{cr} \quad (11)$$

Where  $I_e$  = the beam effective moment of inertia;  $I_{cr}$  = the moment of inertia of the cracked transformed section;  $I_g$  = the moments of inertia of the transformed gross section;  $M_{cr}$  = the moment at first cracking; and  $M_a$  = the maximum moment in the beam at any load stage.

## VALIDATION OF THE ANALYTICAL APPROACH METHOD

### Room Temperature tests

To demonstrate the application of the above procedures, an experimental investigation previously tested by Aiello [3] is analysed by the approach slice method. The beams span length were typical 3,000 mm with a rectangular cross section of 150mm wide and 200 mm high. Two beams were investigate under the following conditions:

- Case 1 refers to beam with hybrid reinforcement steel and AFRP placed on two levels.
- Case-2 refers to beam reinforced with AFRP and steel rebars placed at the same level.

Results obtained using the approach slice method are close to the experimental results obtained for the hybrid reinforced concrete beams. Figure 6 shows good agreement between the approach method and the experimental results.

### Fire tests

Two simply supported beams were tested under fire condition. The specimens were first loaded to a certain percentage of their maximum load capacity (72% for beam FS1 and 81% for beam FS2) and then the fire sequence started. The beams were heated by controlling the temperature in the furnace, this temperature was assumed to follow a predefined heating curve. The span of the beams (between supports) was 2000 mm and the loads were positioned at 700m from each support (4 point loading). Figure 7 illustrates the details of the cross-section of the beams.

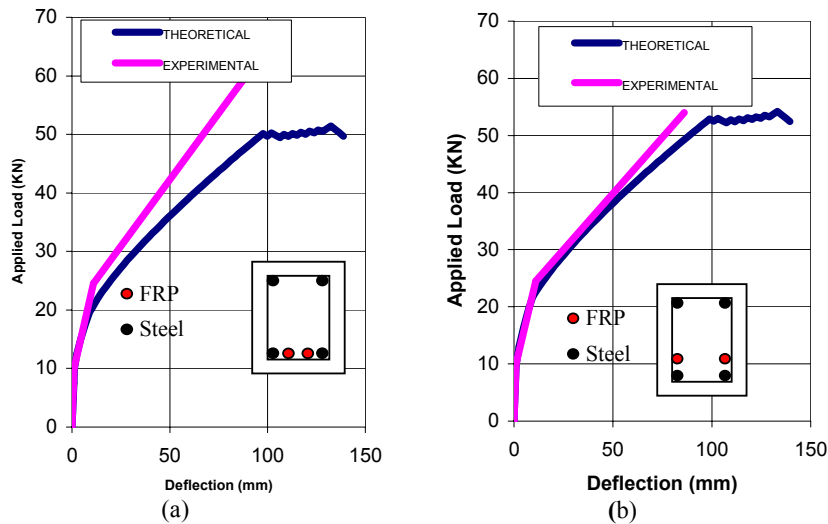


Figure 6. Experimental and theoretical comparison

The bending moment capacity of the section has been calculated as a function of time according to the temperatures recorded during the fire test. It can be seen from Figure 8 that the bending moment capacity of the cross section did not decrease significantly before 15 minutes. The reason is that the steel reinforcement did not reach 400°C before that time, the yield strength ( $\sigma_y$ ) is not significantly affected by temperature below 400°C, and the temperature of the upper part of the beam was still cold enough (less than 100°C).

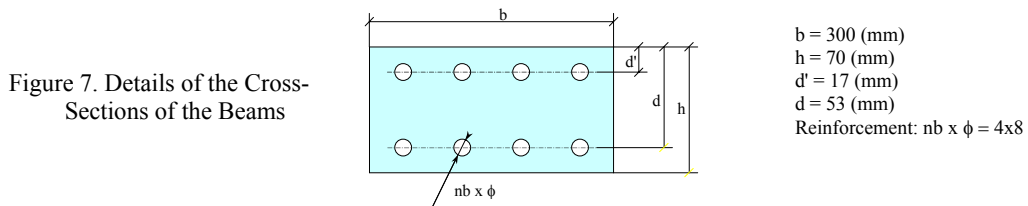


Figure 7. Details of the Cross-Sections of the Beams

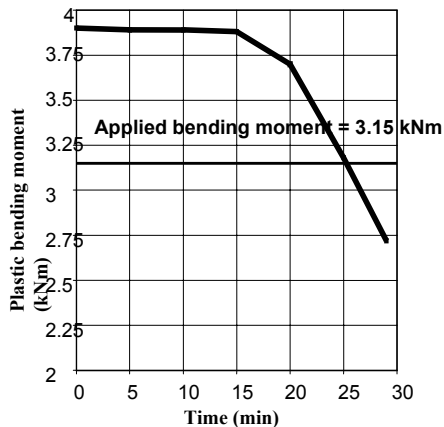


Figure 8. Bending Moment Capacity - Time Diagram

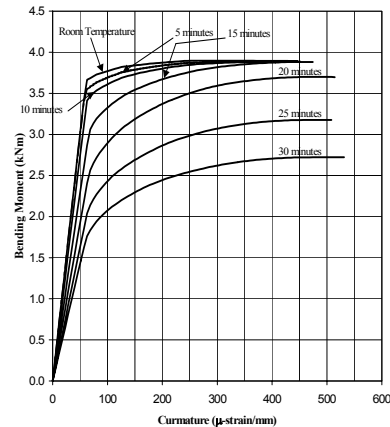


Figure 9. Bending Moment - Curvature Diagram.

After 20 minutes the load bearing capacity of the beam decreased dramatically (Figures 8 and 9), mainly because of the increase in the temperature of the steel reinforcement and by ensuing decrease of its mechanical properties. Figure 8 shows that predicted failure time by the program is between 25 and 26 minutes, this is in good correlation with the experimental failure time that occurred after 24 minutes during the fire test SF2. Concerning the test SF1, failure occurred after 25 minutes and the program predicts a failure time of 27

minutes. Table 1 illustrates the comparison of failure times results between the tests obtained and the theoretical approach method.

Table 1. Comparison of the failure time between experiment and calculation.

	$T_{test}$ (min)	$T_{prog}$ (min)	Load ratio (%)
FR1	24	25.3	72
FR2	25	27	81

Figure 9 shows the curvature-bending moment diagram. Up to 15 minutes the maximum bending moment does not decrease (3.89 kN.m). For a given load level (for example 3.5 kNm) the curvature will be greater after 15 minutes than at room temperature. As mid span curvature is increased from 60 to 135, the deflection at mid span of the beam is also increased. This is in accordance with the phenomenon observed during the fire tests.

### PARAMETRIC STUDY

The beam (Case 1) with hybrid reinforcement steel and AFRP placed on two levels was used to study the effect of fire time exposure and the concrete cover on the FRP temperature. Two types of cover are considered, 25 mm and 50 mm, using concrete with a compressive strength equal to 35 Mpa. Figure 10 illustrates the cross sections of the two beams considered in the parametric study.

Table 2 illustrates the material information used in this investigation, which was previously used by Saafi [21].

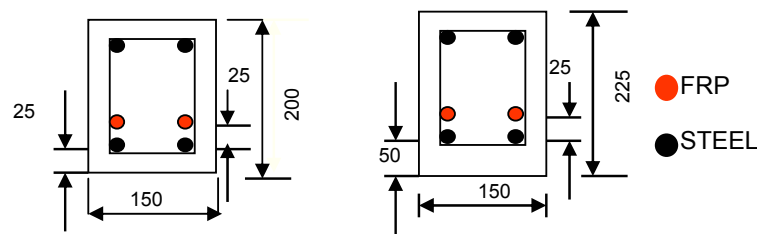


Figure 10. Beam cross sections with different covers

Table 2. Material properties

Material	Ultimate tensile strength (Mpa)	Modulus of Elasticity (Gpa)
GFRP	600	42
AFRP	1200	83
CFRP	2070	152
Steel	414	200

Figures 11-13 show the loads versus the displacement for different times and concrete covers. It can be seen that concrete cover equal to 25 mm has a big effect on the hybrid-steel reinforced beams from fire time 10 min and over. As shown in Figures 11-13, the effect of elevated temperatures on behaviour of FRP reinforced beams is apparent from the continuing decrease in the load capacity of members with time. This degradation is proportional to the change in the properties of reinforcing FRP due to elevated temperatures. Due to the low mechanical properties of GFRP, the degradation of the load capacity of the GFRP reinforced concrete beam is more pronounced than CFRP and AFRP reinforced concrete beams.

The beams had small failure loads with a large deflections; example at fire time equal to 10 minutes the failure loads for AFRP, CFRP and GFRP are respectively: 17kN, 38kN and 13kN. But once, the cover is increased to 50mm the loads increases to 65kN, 80kN and 39 kN for AFRP, CFRP and GFRP respectively. It can be seen that a small addition of cover makes an increase of failure load almost 50 % compared to a cover used of 25 mm. The hybrid steel reinforcement beam with CFRP bars exhibits better performances than AFRP, GFRP; example at 30 minutes the failure load for beam reinforced with CFRP is equal to 71kN compared to AFRP and GFRP which are 50kN and 31kN as given in the order. Figure 13 shows that once the beam reaches the failure load the FRP reinforced bars have completely lost their strength. The beam recovered its strength at certain loads, due to the steel bars and the concrete layer left in the cross section.

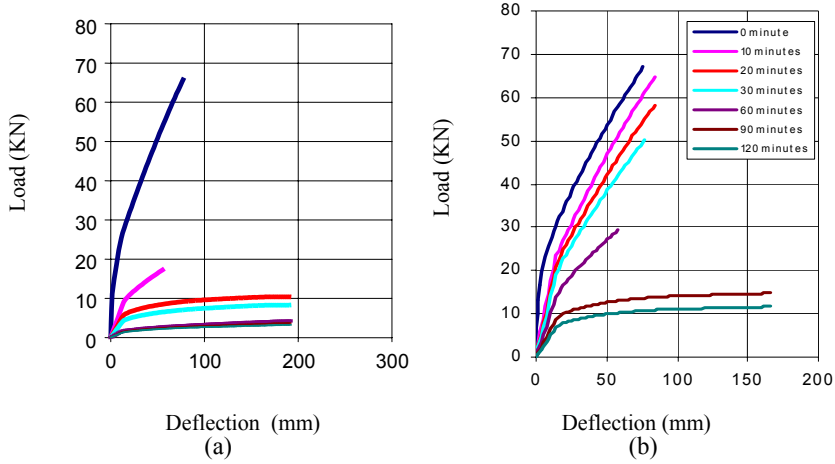


Figure 11. Load deflection curves for beams reinforced with steel and AFRP: (a) cover 25mm, (b) cover 50mm

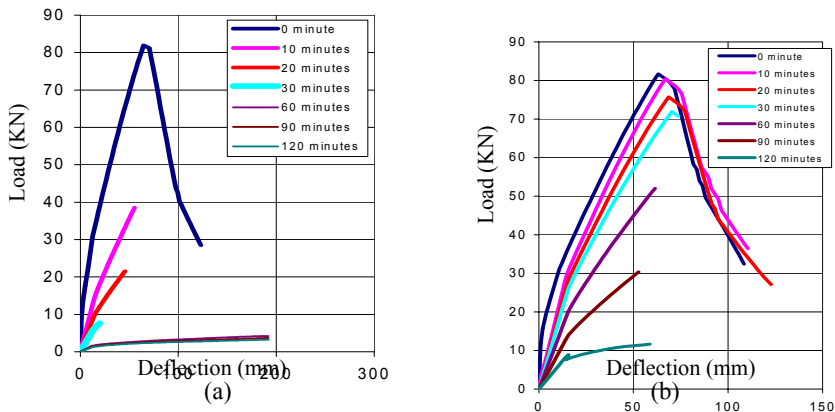


Figure 12. Load deflection curves for beams reinforced with steel and CFRP: (a) cover 25mm, (b) cover 50mm

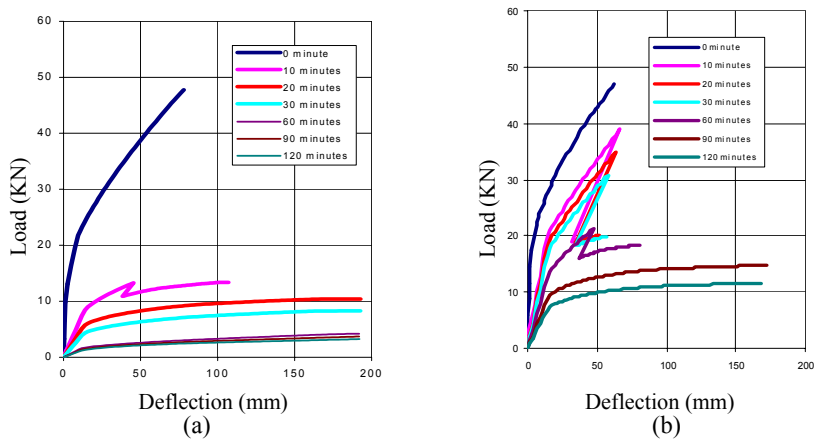


Figure 13. Load deflection curves for beams reinforced with steel and CFRP: (a) cover 25mm, (b) cover 50mm

## CONCLUSIONS

The analytical approach method reported in this paper has shown a good agreement with experimentally available tests at ambient or elevated temperatures. Based on the FRP and concrete properties at elevated temperatures, the failure load and the deflection can be determined. The analytical results have shown that fire exposure has a significant effect on the behaviour of FRP reinforced concrete and its failure load. It was found that the response of FRP reinforced concrete beams depends mainly on the concrete cover. Due to rapid deterioration of FRP reinforcement, Hybrid FRP and steel reinforced concrete beams exhibit greater degradation in flexural resistance than the steel reinforced concrete. It was also found that the minimum concrete cover for hybrid steel reinforced beams is equal to 50 mm. The proposed method is applicable to any type of beam cross section but as further a requirement the effect of shear should be added into consideration.

## REFERENCES

- Abbasi A., and Hogg, P.J., Fire Testing of Concrete Beams with Fibre Reinforced Plastic Rebar, Queen Mary, University of London, Department of Materials, London E1 4NS, 2003.
- Abu-Tair, A.I., Nadjai, A., New Method for Evaluating the Surface Roughness of Concrete for Repair or Strengthening, *International Journal of Construction and Building Materials*, V.14, 171-176, 2000.
- ACI Committee 440. Guide for the design and construction of concrete reinforced with FRP rebars 2001.
- Aiello, M.A. and Ombres, L., "Structural Performances of Concrete Beams with Hybrid (Fibre-Reinforced polymer-Steel) Reinforcements." *Journal of Composites for Construction*, Vol. 6, No. 2, pp. 133-140. 2002.
- Balafas, IG., Burgoyne, C.J., Economic Viability of FRP in Concrete Structures, ConFibreCrete, Web-site: [www.shef.ac.uk](http://www.shef.ac.uk), 2001
- Blontrock H, TaerweL, Matthys S. Properties of fiber reinforced plastics at elevated temperatures with regards to fire resistance of reinforced concrete members. 4 th International Symposium on Non-Metallic (FRP) Reinforced concrete structures, Baltimore, American Concrete Institute (ACI), 1999, pp.43-54.
- Burgoyne, C.J., "Should FRP be Bonded to Concrete." *Fiber-Reinforced-Plastic Reinforcement for Concrete Structures: International Symposium*, Detroit: American Concrete Institute, pp. 367-380, 1993
- Desai, S., 'Design of Reinforced Concrete Beams Under Fire Conditions' *Magazine of Concrete Research*, 50, no. 1, 1998.
- Eurocode 2: Design of concrete structures, 1992. ENV EC2.
- Fujisaki T., Research and Development of Grid Shaped FRP Reinforcement. Nanni A, Dolan C, editors. *Int. Symposium on Fiber Reinforced Plastic Reinforcement for Concrete Structures*. ACI SP-183,. pp. 177-92, 1993
- Lin T.D., Ellingwood B. and Piet O. Flexural and shear behaviour of reinforced concrete beams during fire tests. US Department of Commerce, National Institute for Science and Technology, Centre for Fire Research, Gaithersburg, MD, 1988, nbs-gcr-87-536.
- Nakagawa H. Application of three-dimensional fabrics reinforced concrete to building panel. Nanni A, Dolan C, editors. *Int. Symposium on Fiber Reinforced Plastic Reinforcement for Concrete Structures*, SP-183.pp. 211-32, 1993
- O'Connor, D.J., and Scotney, B.W., 'Determination of Equivalent thermal Response Parameters for Evaluating the Structural Response of Beams Subjected to Transient Thermal Environments', *International Journal of Mathematical Education in Science and Technology*, 26, no. 1, 1995.
- Saafi, M., "Effect of Fire on FRP reinforced Concrete Members", *Composite Structures*, 58, No. 1,pp. 11-20, 2002
- Saafi, M., Effect of fire on FRP reinforced concrete members, *Journal of Composite Structures*, 58, 2002, pp. 11-20.
- Sakashita M., Deflection of continuous fiber reinforced concrete beams subjected to loaded heating. *Non-metallic (FRP) reinforcement for concrete structures*, Japan Concrete Institute, vol. 2, pp. 51-58, 1997
- Sakashita, M., and al., Deflection of Continuous Fiber Reinforced Concrete Beams Subjected to Loaded Heating, *Non-Metallic (FRP) Reinforcement for Concrete Structures*, *Proceedings of the Third International Symposium*, Vol. 2 ,Oct., 1997, pp. 51-58.
- Somboonsong, W., Ko, F. K., and Harris, H. G., "Ductile hybrid fiber reinforced plastic (FRP) rebar for concrete structures: design methodology," *ACI Materials Journal*, 1998.
- Talamona, D, Nadjai, A, Ali, F., Determination of the bending moment capacity of RC beams at ambient and elevated temperatures, *Journal of Applied Fire Science*, Vol. 11(1), 75-90, 2003.
- Tanan H., Fire resistance of continuous fiber reinforced concrete. Taerwe L, editor. *Non-metallic (FRP) reinforcement for concrete structures*. RILEM Proceedings 29,pp. 368-75, 1995
- Wang YC, Wong, PMH, and Kodur, V., Mechanical Properties of fibre Reinforced Polymer Reinforcing Bars at Elevated Temperatures, *Designing Structures in Fire*, Baltimore, USA, October 2003.